HHS Public Access

Author manuscript

Metallomics. Author manuscript; available in PMC 2015 November 01.

Published in final edited form as:

Metallomics. 2014 November ; 6(11): 2072–2082. doi:10.1039/c4mt00161c.

Bimodal-hybrid heterocyclic amine targeting oxidative pathways and copper mis-regulation in Alzheimer's disease

Paulina Gonzalez[a], **Viviana C.P. da Costa**[a], **Kimberly Hyde**[a], **Qiong Wu**[b], **Onofrio Annunziata**[a], **Josep Rizo**[b], **Giridhar Akkaraju**[c], and **Kayla N. Green**[a]

[a]Department of Chemistry, Texas Christian University, 2800 S. University, Fort Worth, USA.

[b]Department of Biophysics, University of Texas Southwestern Medical Center, 5323 Harry Hines Boulevard, Dallas, TX 75390.

[c]Department of Biology, Texas Christian University, 2850 S. University, Fort Worth, USA.

Abstract

Oxidative stress resulting from metal-ion misregulation plays a role in the development of Alzheimer's disease (AD). This process includes the production of tissue-damaging reactive oxygen species and amyloid aggregates. Herein we describe the synthesis, characterization and protective capacity of the small molecule, lipoic cyclen, which has been designed to target molecular features of AD. This construct utilizes the biologically compatible and naturally occurring lipoic acid as a foundation for engendering low cellular toxicity in multiple cell lines, radical scavenging capacity, tuning the metal affinity of the parent cyclen, and results in an unexpected affinity for amyloid without inducing aggregation. The hybrid construct thereby shows protection against cell death induced by amyloid aggregates and copper ions. These results provide evidence for the rational design methods used to produce this fused molecule as a potential strategy for the development of lead compounds for the treatment of neurodegenerative disorders.

Introduction

Alzheimer's disease (AD) is the most common form of dementia afflicting over 11 million individuals worldwide with this number expected to double by 2050.[1] One common feature of AD is unabated inflammation in the form of reactive oxygen species (ROS) in brain tissue. The production of ROS can come from the interaction of mis-regulated metal ions generating the buildup of amyloid (Aβ) plaques and depletion of natural antioxidants in the brain tissue of the afflicted patient. This combination of ROS and Aβ accumulation leads to the death of neurons and loss of cognitive function.[2]

Although transition metal ions play essential roles in human health, ion mis-regulation has been shown to result in interactions between amyloid and redox active metals. Higher levels of metal ions, specifically Cu and Zn, are known to catalyze the formation of amyloid

Electronic Supplementary Information (ESI) available: Cell Viability and rescue studies, ^{15}N results and details of binding studies. See DOI: 10.1039/b000000x/

plaques and have been found in higher concentrations in the tissue of AD patients compared to tissue from brain of non-AD afflicted donors.[3] This has been shown to result in the formation of the toxic fibrils derived from amyloid aggregation and generation of reactive oxygen species (ROS) by Fenton type chemistry, amongst other proceses.[4] Overall this evolving hypothesis proposes an imbalance in Aβ production/clearance, with metal ion mis-regulation, and ROS playing a pivotal role in the development of AD. This cascades into a series of molecular events including gliosis, inflammation, and over-potentiation leading to excitotoxicity, plaques, tangles, oxidative stress, synaptic and neuronal dysfunction which ultimately and synergistically converge and result in the memory loss and dementia exhibited in patients.[5]

Advances are continually being made in the understanding of how ROS and Aβ accumulation is linked to neurodegeneration.[6] Specifically, whether the soluble fibrils and/or insoluble oligomers of Aβ are responsible for the progression of the disease remains one of the major controversies with respect to this model. The former circumstance has gained traction thanks to recent work which has elucidated the early processes that lead to formation of toxic oligomeric species prior to mature fibril aggregation.[6] Regardless, the generation and uncontrolled mitigation of ROS is a concomitant outcome of amyloid aggregation.[4a, 4c, 7] Understanding these pathways gives synthetic chemists targets at which to aim rational synthetic approaches toward producing small molecules capable of modulating these factors.

One therapeutic strategy aimed at abating AD involves the use of metal-ion binding molecules that can restore the metal homeostasis in the brain. These can be categorized according to the following functionalities: (1) antioxidant hybrid molecules, (2) Aβ targeting and (3) enzyme inhibiting activity.[8] Our group has previously studied hybrid molecules composed of a chelator moiety in conjunction with a pyridol functionality which we showed to be responsible for protection against reactive oxygen species in cells.[9] Our studies demonstrate that the fusion of functional groups can engender the positive characteristics of the parent molecules onto the product system. However, they have been largely hindered for *in vivo* work by solubility and biocompatibility. Herein we take a novel approach to the molecular design of agents targeting features of AD by fusing naturally occurring antioxidant constructs to metal binding moieties.

Lipoic acid can act as a coenzyme in metabolic routes of cells, including glutathione synthesis, the most important natural antioxidant in the brain.[10] There have been several *in vitro* studies suggesting that α-lipoic acid (LA) and its reduced form dihydrolipoic acid (DHLA) can inhibit the formation of amyloid fibrils (fAβ), as well as destabilization of preformed fAβ.[11] Here, we integrate lipoic acid into the metal binding cyclen (1,4,7,10-tetraazacyclododecane) scaffold that our previously reported systems resemble based on the metal binding heterocyclic core.[9] This new system is designed to utilize the lipoic acid component to provide multiple modes of ROS targeting activity while tuning the metal binding capacity of the metal-scavenging cyclen core. We report, an array of *ex vivo* and *in vitro* experiments that are carried out to deduce the ability of the water soluble, hybrid lipoic cyclen (**1**) molecule (Figure 1) to modulate amyloid aggregation and oxidative stress while increasing biocompatibility of the original scaffold, cyclen. Most relevant to this work are

cellular assays (utilizing HT-22 neuronal cells) which indicate that **1** can combat cell toxicity induced by amyloid in the presence or absence of copper.

Experimental

General Methods

All reagents used were obtained from commercial sources and used as received, unless noted otherwise. ^{1}H NMR spectra were obtained on a 400-MHz Bruker spectrometer, using deuterated solvents ($CDCl_3$, D_2O) with tetramethylsilane as internal reference (in parts per million; Me_4Si, δ = 0.00 ppm). ^{13}C NMR spectra were obtained at 100-MHz using $CDCl_3$ as internal reference (δ = 77.36 ppm). For proper identification of the NMR signals the following abbreviations were used: s = singlet, d = doublet, t = triplet, m = multiplet. When noted, purification of the compounds was accomplished with flash chromatography using silica gel (63–200 μm). TLC plates were developed using iodine and UV light, when possible. Electronic absorption spectra were recorded on a DU 800 UV-Vis spectrophotometer (Beckman Coulter) using a 1 mL quartz cuvette with a 1 cm path length or a Molecular Devices Kinetic Microplate Reader for colorimetric assays. ESI-MS experiments were carried out using an Agilent 6224 Accurate-Mass Time-Of-Flight (TOF) MS. HPLC chromatograms were obtained using a C8 reversed phase column, unless noted otherwise, with 100% MeOH at a flow rate of 0.5 mL/min on an Agilent 1100 series instrument, which was coupled to Bruker Daltonics Esquire 6000 ESI-MS. Preparation of dibenzyl 1,4,7,10-tetraazacyclododecane-1,7 dicarboxylate (**3**) was produced according to a method by De Leon *et al.*[12]

Synthesis. (±)-5-(1,2-dithiolan-3-yl)pentanoyl chloride (2)—To a stirred solution of thionyl chloride (1.4 mL, 7.5 mmol) in CH_2Cl_2 (30 mL) at 0°C was added a CH_2Cl_2 solution of lipoic acid (3.0 g, 5 mmol), dropwise over 1 h. The mixture was allowed to stir for an additional 3 h at the same temperature. The solvent was removed under vacuum (without any heating) and used without further purification in the next step. The reaction proceeded with quantitative yield.[13] ^{1}H NMR (400 MHz, $CDCl_3$): δ[ppm] = 1.519 (m, 2H), 1.670–1.776 (m, 4H), 1.905 (m, 2H), 2.464 (m, 1H), 3.157 (m, 2H), 3.567 (p, 2H).

Preparation of the dibenzyl 4-(5-(1,2-dithiolan-3-yl)pentanoyl)-1,4,7,10-tetraazacyclododecane-1,7-dicarboxylate (**4**). To an ice bath cooled solution of **3**[12] (5.8 g, 5.7 mmol) and triethylamine (5.6 mL, 40.1 mmol) in CH_2Cl_2 were continuously added dropwise to the prepared solution of **2** (3.0 g, 13.3 mmol) in CH_2Cl_2. The reaction mixture was stirred overnight. The mixture was washed with the series of a saturated solution of sodium bicarbonate, 1 N HCl, brine and then dried over Na_2SO_4. The resulting solution was filtered and the solvent was then removed under reduced pressure. The crude product was purified by gradient column chromatography with an eluent from EtOAc to 5% MeOH : EtOAc resulting in a yellow oil: 56% isolated yield. ^{1}H NMR (400 MHz, $CDCl_3$): δ[ppm] = 1.20–1.40 (m, 2H), 1.41–1.59 (m, 2H), 1.61–1.82 (m, 2H), 1.83–1.95 (m, 2H), 1.99–2.12 (s, 1H), 2.34–2.52 (m, 1H), 2.63–2.92 (m, 2H), 2.95–3.06 (m, 2H), 3.47–3.89 (m, 16H), 5.03–5.23 (s, 4H), 7.22–7.47 (m, 10 H); ^{13}C NMR (100 MHz, $CDCl_3$): δ[ppm] = 29.0, 32.1, 34.9, 38.5, 40.3, 42.7, 46.3, 47.8, 50.6, 56.4, 67.1, 128.2, 136.4, 156.5, 172.6; MS (ESI,

$CH_3CN:H_2O$ + 0.1% CH_2O_2) Theoretical = 629.2831 $[M+H]^+$, Experimental = 629.4598 $[M+H]^+$.

Preparation of 5-(1,2-dithiolan-3-yl)-1-(1,4,7,10-tetraazacyclododecan-1-yl)pentan-1-one (1)—Boron trichloride in CH_2Cl_2 (1 mL, 8.5 mmol) was carefully added to a previously purged flask with nitrogen, containing **4** (1.2 g, 1.9 mmol). The white suspension was then allowed to stir for 24 h. Excess CH_2Cl_2 was removed under reduced pressure. To the resultant yellow solid, MeOH was added carefully and rotavaped down (3×). The residue was resuspended in water and HCl was added, and the aqueous layer washed with EtOAc, and lyophilized to yield the product as a yellow solid in 89% yield. mp 195°C-198°C. ^{1}H NMR (400 MHz, $CDCl_3$): δ[ppm] =1.27–1.76 (m, 7H), 1.76–2.15 (m, 2H), 2.25–2.53 (m, 2H), 2.71–2.95 (m, 2H), 2.97–3.45 (m, 14H), 3.47–3.82 (m, 5H); ^{13}C NMR (100 MHz, $CDCl_3$): δ[ppm] =24.2, 28.1, 33.5, 38.0, 40.3, 43.0, 43.7, 44.7, 46.2 , 47.1, 56.5, 172.0; MS (ESI, $CH_3CN:H_2O$ + 0.1% CH_2O_2) Theoretical = 361.2096 $[M+H]^+$, Experimental = 361.2710 $[M+H]^+$.

Copper Binding studies—Aqueous stock solutions were prepared by weight for both ligands: **1** and cyclen. The molar concentrations of these solutions were 16.7 mM and 12.8 mM for **1** and 10.2 mM for cyclen. A copper nitrate aqueous stock solution with a molar concentration of 33.4 mM was also prepared by weight. Deionized and ultra-pure water was obtained from a four-stage Millipore filter system and used to prepare all solutions. Copper-ligand solutions for spectroscopy measurements were obtained by mixing known amounts of copper and ligand stock solutions. The copper concentration was kept constant at 3.4 mM for all the samples. A 0.10-M acetate buffer (pH = 5.0) was also added so that the final buffer concentration was 0.01 M. To approximately maintain a constant ionic strength , a 1.0-M solution of sodium nitrate was also added so that its final concentration was 0.10 M. The absorption spectroscopy measurements were made on a UV-vis DU 800 spectrophotometer (Beckman Coulter) using a 1-cm path length cuvette, at room temperature. The obtained results are reported as normalized absorption spectra by calculating the molar absorption coefficient, ε, with respect to the copper concentration, C_M. In the absence of ligand, the absorption spectrum of the copper salt shows a weak band with a maximum at the wavelength (λ_{max}) of 770 nm. Note that λ_{max}=810 nm corresponds to the hydrated $[Cu(H_2O)_6]^{2+}$ species. The observed blue shift can be related to the complex formation between copper and acetate ions (formation constant, $\beta=4\times10^3$, 25 °C). A stronger shift was observed in the cyclen case. This can be attributed to a corresponding stronger binding interaction with copper ions and is consistent with reported binding studies.[14]

Biological methods—For the biological assays, HT-22 neuronal cell line from mouse hippocampus (passages 10–20) was used and incubated at 37°C in a 5% CO_2 humidified atmosphere in Dulbecco's Modified Eagle Medium (500 mL) containing 100units/mL penicillin/ 100μg/mL streptomycin 100× (5 mL), 2 mM Glutamine (100 mM, 5 mL), and charcoal stripped fetal bovine serum (15%). To prepare dilutions of compounds the same media was used excluding the addition of the serum and antibiotics. Human Embryonic Kydney (HEK 293) cells were used as a control cell line and were maintained in a maner similar to the HT-22, using regular FBS instead of charcoal stripped.

Amyloid-β (Aβ) Peptide Experiments $Aβ_{1–40}$ Preparation—For all the Aβ experiments, $Aβ_{1–40}$ (21st Century Biochemicals) was used as the ammonia salt, obtained by dissolving Aβ in chelex-treated milliQ water (treated overnight) , prepared as a 1% v/v solution of NH_4OH to yield a final concentration of 200 μM, divided into aliquots, lyophilized and stored at −80°C until use.

MTT Assay—Cells were seeded in a 96 well plate at a density of 5000 cells per well (in 100 μL complete medium). After 24 h cells were treated with compounds, Aβ, Cu^{+2}, or a combination, and incubated for 48 h at 37 °C. After the incubation time, media was discarded and cells were then treated with 100 μL of 3-(4,5-dimethylthiazol-2-yl)-2,5-diphenyltetrazolium bromide (MTT) (1 mg/1 mL in serum free media) and incubated for 4 h at 37 °C. Media was discarded and the formazan precipitate solubilized in 100 μL of DMSO, rocked for 5 minutes and the absorbance (A_{540}) was measured using a Molecular Devices Kinetic Microplate Reader; the data obtained was processed using MasterPlex 2010 software for EC_{50} calculations and Stat View for the ANOVA tests.

DPPH assay—A 2,2-diphenyl-1-picrylhydrazyl (DPPH) stock solution was prepared by dissolving 25 mg of DPPH solid in 100 mL of absolute EtOH. The working radical solution was prepared by dilution with absolute EtOH to an absorbance of 1.3 at 512 nm. Stock solutions of the compounds tested were dissolved in deionized H_2O and EtOH 95% for the BHT solutions respectively and serial dilutions were made to get different concentrations. For the analysis 2 mL of the solutions were incubated with 2 mL of DPPH working solutions in the dark for 24 h as well as 2 mL of DPPH working solution with 2 mL of H_2O or EtOH to serve as blank. Analysis of the solutions was performed as follows: 1 mL of the sample solution was diluted with 1 mL of H_2O shaken and the absorbance was measured at 515 nm.

Determination of Amyloid aggregation based on Transmission Electron Microscopy (TEM)—Samples for transmission electron microscopy were prepared using a 15 μM solution of Aβ dissolved in milliQ water previously treated with chelex, 30 μM $CuCl_2$ and 50 μM **1** respectively, incubated overnight at 37°C with continuous agitation and centrifuged before applying them to the grids taking the bottom part of the solution. Glow discharged grids (Formar/Carbon coated 200 mesh, Electron Microscopy Sciences) were treated with one drop from the different solutions for 5 minutes at room temperature. Excess of sample was removed with a filter paper and washed three times with doubly distilled H_2O, stained with 1% uranyl acetate for 15 minutes, excess of uranyl acetate was absorbed with a filter paper, samples were dried at room temperature and analysed with a JEOL 2100 at 200 kV, 8 k magnification.

Tyr-10 Intrinsic Fluorescence Assay—Solutions containing a final concentration of 15 μM Aβ, 30 μM $CuCl_2$ and 50 μM **1** were respectively dissolved in 1X PBS, following this order of addition: compound, peptide, copper. Following incubation for 1 hour at 37°C, fluorescence intensity was measured (Ex_{270}, Em_{290}). Each measurement was made in triplicate. Note: Several factors should be considered when working with amyloid protein for studies such as this. Aggregation of Aβ can occur in several stages and therefore

solutions are generally not very stable for long periods of time. Studies following Aβ aggregation by fluorescence involve the monomerization of any previous aggregate formed in the peptide with hexafluoroisopropanol (HFIP). Kinetic studies following aggregation of Aβ have shown the same results of amyloid aggregation with and without treatment with HFIP within one hour after the reactions have started. However after that hour, the solution without HFIP becomes unstable.[15] Therefore the approach here presented is based analysing only the first hour of incubation of the protein, avoiding one extra element (HFIP) that could interfere with aggregation and solubilisation of the protein as well with the interaction of this solvent with the intrinsic fluorophore tyrosine.

Determination of Amyloid aggregation based on Native gel electrophoresis with Western Blotting—Solutions prepared for the Tyr-10 fluorescence assay were analysed by native gel electrophoresis with Western Blotting using anti-Aβ (6E10) as primary antibody. Each sample contains 15 μM Aβ, 30 μM of $CuCl_2$ and 50 μM of **1** respectively as well as a sample of Aβ 15 μM containing SDS as a control for the monomeric species, were separated using a 10 – 20% Tris-tricine gradient gel (Invitrogen). The gel was transferred to a PDVF membrane (1h, 100v, 4°C) and blocked overnight with a solution of 3% w/v bovine serum albumin (BSA) dissolved in Tris-buffered saline containing 0.1% Tween 20 (TBST), the membrane was treated with primary antibody 6E10 (1:1000; 2% BSA in TBS-T, Covance) for 4 hours at room temperature. The membrane was then incubated with the horseradish peroxidase-conjugated goat anti-mouse antibody (1:10000) in 2% BSA in TBS-T for 1 hour at room temperature. The Thermo Scientific Supersignal West Pico Chemiluminescent Substrate was used to visualize protein bands.

Two-dimensional (2D) 1H–15N Heteronuclear Single Quantum Correlation (HSQC) NMR measurement—Uniformly ^{15}N-labeled Aβ1–40 was purchased from rPeptide, prepared as described in the Aβ experiments, aliquoted and stored at −80°C until use. The NMR sample was made from stock solutions with the following concentrations: 100 μM ^{15}N labeled Aβ1–40, 0.1 M potassium phosphate buffer pH 7.3, 1 M NaCl, 14.27 mM **1**. The final samples are in 20 mM of potassium phosphate buffer, pH 7.04 with concentration of 20 μM and D_2O (7% v/v), and the rest of the volume was completed with ddH_2O or 1.5 equivalents of **1** were added. Samples co-incubated with **1** were allowed to mix for 5 minutes prior to the experiment. ^{1}H- ^{15}N HSQC experiments were carried out at 5°C on a 800 MHz Varian Inova system, equipped with cold probe, with 9600 kHz and 1800 kHz spectral width and 1640 and 80 complex data points in the ^{1}H and ^{15}N dimension respectively. Scans (32) for each t_1 experiment and 1.5 seconds recycle delay.

Docking Studies of 1 with AutoDock Vina—Docking studies of 1 or cyclen were performed using a previously determined NMR model of Aβ1–40 obtained in an aqueous solution (PDB 2LFM) and previously used for metal chelator analysis. 16 Out of 20 conformations reported in the PDB file, the one that correlated better with the 2D NMR studies was selected. The ligand structure was optimized for the docking studies in ChemBio3D Pro 12.0 with the MM2 energy minimization. AutoDock Tools was used to prepare Aβ protein optimized structural files that were run with AutoDock Vina using PyRx to obtain the binding energies. The search space dimensions were selected in order to

contain the entire peptide with an exhaustiveness of 1024 runs. The visualization of the docking results were made using PyMol.

Discussion

Design and Synthesis of 1

Molecule **1** contains the biological antioxidant, lipoic acid, tethered to a metal binding domain, cyclen. The addition of lipoic acid to this construct abates the oxidative stress that has been shown to modify proteins, lipids and DNA resulting in unstable or less functional systems and giving rise to mutations. We therefore set out to fuse the natural antioxidant lipoic acid onto a well-characterized Cu^{2+} chelator (cyclen). This design targets known molecular assaults associated with AD: mis-regulated metal ions alone and those interacting with amyloid, along with targeting ROS generation.

Molecule **1** was converted from a high-affinity system (cyclen) to a moderate metal binding structure via an acyl linkage to lipoic acid utilizing a straightforward methodology involving three steps (Scheme 1). Specifically, the synthesis of **1** begins with the protection of 1,7-amines of cyclen with benzyl chloroformate following previously reported methods.[12] Concurrent conversion of lipoic acid to lipoic chloride with thionyl chloride in dichloromethane proceeds smoothly in quantitative yield. These two products are then combined to react in the presence of triethylamine to form an amide bond in position-10 of cyclen through a nucleophilic substitution at the carbonyl group. Di-substitution of cyclen with lipoic chloride is observed as trace products and can be separated using column chromatography. Finally, deprotection of the Cbz group with boron trichloride gave the desired product. The HCl salt of **1** was isolated as a water soluble yellow powder, stable to the atmosphere for long periods of time.

Copper binding of cyclen is attenuated by addition of lipoic acid

The main antioxidant defense of the cell against ROS is primarily the copper containing enzyme superoxide dismutase I. Therefore, copper metabolism inside the cell is an interesting aspect considering that either the overload or deficiency of this metal will result in an oxidative challenge in terms of cellular health.[17] Moreover the brain is particularly susceptible in the case of copper mis-regulation because it is highly sensitive to oxidative stress as a consequence of a variety of factors. Furthermore copper uptake in the cell is strongly influenced by glutathione levels, it is important to consider that glutathione is a copper chelator as well as a natural antioxidant in the brain, thus playing an important role in the generation of ROS.[18] Therefore the design of a small molecule targeting metal ions must involve careful tuning of the metal binding core to avoid disturbing the natural homeostasis of copper inside the cell.

Spectrophotometric methods for determination of the binding affinity of **1** were carried out to verify that the acyl group of the lipoic acid tunes down the tight-binding affinity of cyclen for copper.[14] Figure 2 shows normalized absorption spectra of aqueous copper(II) solutions in the presence of cyclen (figure 2a) and **1** (figure 2b). These spectra were obtained as a function of ligand concentration at constant copper(II) concentration. For the molecules

investigated, cyclen and **1**, λ_{max} shifts towards shorter wavelengths, compared to the copper starting material, as ligand concentration increases and approaches a saturation value at high ligand concentration; λ_{max} = 590 nm and 670 nm for cyclen and **1** respectively. Both complex binding constant (K/mM^{-1}) values were determined using a fitting function based on the relative change of copper absorption coefficient, $\varepsilon/\varepsilon_0$, with respect to the ligand-copper molar ratio (C_L/C_M), where ε_0 is the absorption coefficient of copper in the absence of ligand (details in SI). The extracted values are reported in Table S3. The results, presented in Figure 2, support a 1:1 binding stoichiometry for both cyclen (as expected) and **1**. For **1**, a moderate binding of 6.4±1.7 mM^{-1} was calculated for these conditions. For cyclen, however, our experimental data cannot be used to extract K because of very strong binding between cyclen and copper. Nonetheless, the fitting function can satisfactorily describe these data only if K is higher than 10^2 mM^{-1}. Indeed, for the copper-cyclen complex in aqueous solutions with 0.1 M $NaNO_3$ the literature value of K is 1.8×10^{16} mM^{-1}.[14] This is consistent with the expected acyl attachment of **1** reducing the donor capacity of the N-atom in the N-heterocyclic ring thereby lowering the binding capacity. Overall these results indicate that the employed substitution methods provide a controlled tuning of metal-binding affinity as expected. A moderate-weak metal chaperone system like **1** is projected to exhibit smaller perturbations in metal-ion trafficking pathways, making it a more suitable molecule for intracellular activity.

1 has enhanced biocompatibility

For **1** to be suitable as an anti-oxidant and metal binding agent in biological systems it must exhibit minimal toxicity was therefore explored to establish the biocompatibility of this novel hybrid construct as well as define the effects of integrating the lipoic component onto the heterocyclic core. The 3-(4,5-dimethythiazol-2-yl)-2,5-diphenyl tetrazolium bromide (MTT) assay was utilized in order to evaluate **1** for cytotoxicity. The HT-22 neuronal cell line was utilized for this study due to the hippocampal origin (the hippocampus being the center of learning and memory in the brain). Moreover, an increased degenerative effect is observed in this region of the brain in AD patients making this cell line appropriate for these studies. As shown in Figure 3, following incubation of cells for 48 h with 1 nM to 10 mM **1**, an EC_{50} value of 750 μM was derived corresponding to the concentration necessary to elicit toxicity in 50% of cells studied. In comparison, the parent cyclen backbone showed an EC_{50} of 80 μM (Figure S1). This result indicates that **1** is 9.4× less toxic than cyclen alone. This decrease in toxicity is believed to be a result of the addition of lipoic acid to the construct. This increased biological tolerance translates to other cell lines as well. HEK-293 (human embryonic kidney) cells were co-incubated with **1** or cyclen resulting in a ~33% increase in the concentration of **1** required to induce cell death compared to cyclen. This micromolar toxicity provided us with a wide range of concentrations for the studies presented herein and supports an overall biological tolerance for future *in vivo* work.

1 protects against amyloid and Cu^{2+} toxicity in neuronal cell culture

Amyloid has been shown to cause neuronal cell death by a number of pathways upon entering the cell by endocytotic pathways. Given the low toxicity of **1**, the potential of **1** to reduce cell death induced by Aβ was explored. Neuronal HT-22 cells were exposed to Aβ

and a concentration dependent toxicity was observed as shown in Figure 4. A concentration of 15 μM Aβ consistently caused ~20% cell death and was therefore used for subsequent rescue studies using **1** discussed herein. As shown in Figure 4, a single dose of **1** was added in the range of 50 to 120 μM resulting in a concentration dependent response of increased cell viability. This indicated that **1** was capable of restoring cellular health impaired by Aβ. Specifically, the largest protection (17 %) was observed for the samples co-incubated with 120 μM **1**. Statistical significance ($p<0.005$) for samples of 100–120 μM **1** was observed (Figure S2). A small protection against copper induced toxicity was observed for **1** at higher concentrations as well (Figure S3). We did not observe any protection with cyclen at the same concentrations. In fact, an increase in cell death occurred and is consistent with toxicity data of cyclen (Figure S1).

Subsequently identical experimental conditions were carried out with the sequential addition of 15 μM $CuCl_2$ and Aβ. As expected, a decrease in cell viability was observed (37%). The addition of increasing concentrations of **1** to copper treated cells (Figure 4) showed a statistically significant ability to protect against Aβ+Cu^{2+} induced toxicity in all concentrations studied ($p<0.005$, 50–80 μM; $p<0.05$, 100–120 μM). In fact the 120 μM sample of **1** almost completely restores the viability of cells resulting in a net increase in viability of 34% from the Cu/Aβ treated control, resulting in 97% viability. The results indicate that **1** is a potent rescue molecule capable of abating the combined degenerative effects of copper ions in the presence of amyloid.

Defining the observed therapeutic effect of 1

In order to elucidate the mode(s) of action for the protective capacity of **1**, a gamut of spectroscopic and biological studies were carried out. As stated previously, amyloid and metal ion regulation are closely tied to oxidative stress levels in cells. The result of an imbalance in these species is gaining credence in the metal based hypothesis of AD. The following experiments were designed to dissect the synthetic rationale of **1** and how it relates to the observed protective nature reported above. In addition, amyloid interactions were also explored.

1 acts as a radical scavenger—As radicals are one product of miscompartmentalized metal ions, the radical scavenging capability of **1** was tested using the DPPH assay. BHT (butylhydroxytoluene) was used as a positive control due to its known antioxidant properties. Figure 5 shows that high concentrations (1250 μM) of BHT are capable of quenching 80% of the DPPH radical while cyclen shows no activity. Compound **1** at 1250 μM is equally proficient with BHT at quenching an equivalent amount of radical, following a dose response trend up to 62.5 μM concentration. Comparison of the concentration range of 1250 to 62.5 μM of the radical scavenging capacity of compound **1** with the parent cyclen backbone shows that the activity observed in **1** is improved as a result of the lipoic acid moiety. It should be noted that the concentrations required to quench radicals are parallel to those utilized in the cellular assays reported above and support the hypothesis that **1** could be acting as an intracellular antioxidant via radical scavenging.

Lipoic acid can act as a coenzyme in several metabolic and biosynthetic pathways , including glutathione synthesis. Given the possibility that **1** could be metabolized into glutathione, the major antioxidant defense found within the intracellular domain in the brain, we investigated the possibility of **1** supplementing GSH pathways as a potential mode of action for the protection observed in Figure 4. For this study, HT-22 cells were co-incubated with the small molecule BSO (2-amino-4-(butylsulfonimidoyl)butanoic acid) known to inhibit the synthesis of glutathione in cells. This results in oxidative stress and cellular death as shown in Figure S4.[19] The GSH-Glo™ Glutathione Assay was used to measure GSH levels following **1** addition. The results indicate that GSH levels are depleted in the presence of BSO as expected but are not restored by **1** addition. These results support the conclusion that the **1** molecule does not supplement the GSH antioxidant pathway and likely provides protective capacity via radical scavenging and metal-ion sequestration. [4a, 4c, 7] This hypothesis is further supported by previous work that has shown the LA and DHLA molecules can also act as scavengers for ROS due to a relatively low redox potential (−320 mV). Such studies have also shown cellular protection from ROS generating insults as well.[10a-d, 11, 20]

1 modulates Aβ aggregation induced by Cu^{2+}—A growing consensus relates the toxicity of amyloid to the morphology of the protein in its aggregated form.[6] We therefore set out to explore the effect of **1** on the morphology of aggregated amyloid. TEM can be used to visualize the morphology of proteins, specifically amyloid.[16a] This makes it a powerful tool for understanding the effects of metal-ions on aggregation and the changes induced by small molecules like **1**. For the studies presented herein, a 15 μM amyloid solution was prepared in milliQ water previously treated with chelex. To these solutions, 30 μM $CuCl_2$ and 50 μM **1** were added, respectively, incubated overnight at 37°C with continuous agitation and then centrifuged before applying them to the glow discharged grids and stained. Figure 6a shows the sample containing only Aβ with morphology similar to fibrils reported by others.[16a] Figure 6b shows how the morphology of the protein changes drastically when co-incubated with copper. Finally, Figure 6c shows the solution of Aβ +Cu^{2+}+**1** where the morphology of the protein resembles that of amyloid alone (Figure 6a) indicating that **1** is capable of reconstituting the morphology of Aβ.

Previous studies have shown that the intrinsic fluorescent probe, Tyr-10, in the Aβ protein can be used to track stages of Aβ aggregation.[21] The aggregation of amyloid can be linked to this florescence signal which results from the ability of Tyr-10 to rotate freely. This rotation is impeded upon aggregation resulting in a quenched florescent signal. This assay was utilized to evaluate the effect of **1** upon the aggregation of Aβ. The normalized results shown in Figure 7 correlate with previous reports that addition of copper ions to Aβ results in a decrease in the fluorescence intensity by 56% compared with the sample containing Aβ alone.[21] Addition of **1** to the Aβ + Cu^{2+} system results in the recovery of 23% of the fluorescent signal. For comparison, the parent cyclen molecule showed a complete recovery of Tyr-10 fluorescence signal. Previous studies with small molecule chelators have attributed similar disaggregate activity to the capacity of such molecules extracting metals from Aβ thus disaggregating the protein.[9b] This results in restoration of the Tyr-10 signal. It

is interesting to note that the signal of the **1** did not show equivalent capacity to restore the fluorescence signal.

To corroborate the results obtained with the Tyr-10 assay and the TEM images, polyacrylamide gel electrophoresis under native conditions followed by western blot was used to identify the aggregation level of amyloid as well as the capability of **1** to reduce the aggregate size of the protein. As shown in Figure 8, the amyloid solution aggregates naturally, presumably in fibrilllar forms shown in the previous TEM experiment. The addition of copper to amyloid induces the formation of larger M.W. species of Aβ (seen as an increase in the intensity of the signal toward the top of the lane) which may be correlated to oligomer formation. The addition of **1** results in a reduction of aggregate size (the high M.W. species on the gel image) is observed and correlates with the results obtained with the Tyr-10 fluorescent assay. The same behaviour is shown in the presence of the parent molecule, cyclen, which could be attributed to its copper chelating ability. This is consistent with previously reported literature.[16a, 16c, d, 22]

Two-dimensional (2D) $^{1}H–^{15}N$ heteronuclear single quantum correlation (HSQC) NMR measurements

Based on the aggregation work described above, it was postulated that **1** could be acting in a protective manner via interacting with amyloid in a fashion that prevented aggregation and thus toxicity. Therefore 2D ^{1}H-^{15}N HSQC spectra of uniformly ^{15}N-labeled Aβ in the absence and presence of a 1.5-fold excess of **1** was acquired. The spectra were acquired at low Aβ concentration (20 μM) and 5°C to hinder aggregation. Interestingly, addition of **1** did not induce marked shifts on the Aβ cross-peaks as others have reported[16b] (Figure 9), but did increase the intensities of most cross-peaks (Figure S6). The absence of cross-peak shifts indicates that **1** does not bind directly to monomeric Aβ. However, the increased cross-peak intensities show that **1** must interact somehow with Aβ. A plausible interpretation of these findings is that, without the compound, Aβ has a tendency to oligomerize, and chemical exchange between the monomeric form and oligomers causes broadening of the ^{1}H-^{15}N HSQC cross-peaks of the monomer, which results in decreased cross-peak intensities. Since most of the peptide is involved in the aggregation, all signals are expected to be broadened to some degree. The broadening comes not only from the slower motions of the oligomers but also from chemical exchange between the monomer and oligomers. Chemical exchange will broaden more strongly the signals that have larger chemical shift change between oligomer and monomer, and this is rather unpredictable; hence, it is natural to observe a relatively random distribution of the amount of broadening in the cross-peaks (Figure S6c). In this interpretation, addition of **1** increases the cross-peak intensities because it prevents aggregation, likely by binding to the nascent oligomers and forming a non-productive edge that hinders oligomer growth.

Docking Studies of 1 with amyloid protein

The ^{15}N HSQC results suggested a **1** amyloid interaction. Therefore computational docking studies were carried out to support these in situ results. AutoDock Vina software was utilized in a manner similar to the methods reported separately by Lim and co-workers.[16] Interestingly a moderate amyloid-**1** interaction is supported by a K_d of −5.4 kcal/mol. This is

increased from identical calculations using cyclen which yielded a K_d of −4.1 kcal/mol. These results indicate that the lipoic addition to cyclen correlates to an interaction with amyloid capable of modulating the structure of amyloid as evidenced by these calculations along with the Tyr-10 and HSQC results. Moreover one can also appreciate in fig 10b the interaction of **1** considering the electron density of Aβ which would help to explain the increase of intensity signals in the HSQC experiments, which indicates that affects this binding site of the protein in a manner that prevents its interactions with other monomers, therefore reducing the aggregation process, which translates into more flexible residues in Aβ increasing the signals in the HSQC experiments.

Computational ca1ulations support the potential of 1 having ability to cross the blood brain barrier (BBB)

The potential of **1** to cross the blood brain barrier was assessed by theoretical calculations of Log K_{ow}. The results were obtained using the software EPI suite version 1.68 which uses the atom/fragment contribution method (Moriguchi's method). Systems with log K_{ow} values > 5 are considered to have high bioaccumulation potential similar to Lipinsky's rule of five. Conversely, compounds with low log K_{ow} (<1) will correlate to poor permeation and bio-distribution.[23] Table 2 presents the calculated coefficient values according to the linear and non-linear descriptors from already known compounds following the Moriguchi's rules. The results obtained for the value of log K_{ow} (1.1710) are within the range (log K_{ow} = 1–3) of previously described compounds[24] and support that **1** can potentially cross the BBB. Comparing the results to those obtained with cyclen (log K_{ow} = −1.8270, Table S1) shows that the addition of lipoic acid to this scaffold not only increases bioavailability but also increases the ability of biodistribution across membranes, specifically the blood brain barrier.

Conclusions

The hybrid molecule **1** has shown low toxicity and the ability to protect neuronal cells against death induced by Aβ + Cu, two molecular components associated with the pathology of AD. Molecule **1** is capable of potent antioxidant activity through radical scavenging and moderate binding of copper ions. Moreover, **1** is capable of breaking apart amyloid aggregates as evidenced by TEM images of **1** with amyloid+Cu and interacts with amyloid in a non-aggregate producing manner according to ^{15}N HSQC studies. Overall this work shows that the rationale used to produce the water soluble and air stable compound **1.** This compound can serve as a tool to study the role of Aβ, copper and ROS in neuronal toxicity and could serve as a platform for the development of lead compounds for the treatment of neurodegenerative disorders such as AD.

Supplementary Material

Refer to Web version on PubMed Central for supplementary material.

Acknowledgements

The authors are grateful for generous financial support from the NIH (to J. R., NS037200), TCU Andrews Institute of Mathematics & Science Education (to KG), TCU Research and Creativity Activity Grant (to KG), and the Robert A. Welch Foundation (to KG, P-1760). The authors would like to thank Bruker AXS – Dr. Clemens Anklin and JEOL, Tony Benvenuto along with Wenjing Wu for assistance with Western Blot Training.

Notes and references

1. Alzheimer’s Disease Facts and Figures, Alzheimer’s & Dementia. Alzheimer’s Association. 2011; 7
2. (a) Mathis CA, Wang Y, Klunk WE. Imaging β-amyloid plaques and neurofibrillary tangles in the aging human brain. Current Pharmaceutical Design. 2004; 10:1469–1492. [PubMed: 15134570] (b) Que EL, Domaille DW, Chang CJ. Metals in Neurobiology: Probing Their Chemistry and Biology with Molecular Imaging. Chem. Rev. 2008; 108:1517–1549. [PubMed: 18426241] (c) Gaggelli E, Kozlowski H, Valensin D, Valensin G. Copper homeostasis and neurodegenerative disorders (Alzheimer's, prion, and Parkinson's diseases and amyotrophic lateral sclerosis). Chem. Rev. 2006; 106:1995–2044. [PubMed: 16771441]
3. (a) Lovell MA, Robertson JD, Teesdale WJ. Copper, iron and zinc in AD senile plaques. J. Neurol Sci. 1998; 158:47–52. [PubMed: 9667777] (b) Bishop GM, Robinson SR, Liu Q, Perry G, Atwood CS, Smith MA. Iron: a pathological mediator of Alzheimer disease? Dev Neurosci. 2002; 24:184–187. [PubMed: 12401957] (c) Smith DP, Ciccotosto GD, Tew DJ, Fodero-Tavoletti MT, Johanssen T, Masters CL, Barnham KJ, Cappai R. Concentration Dependent Cu2+ Induced Aggregation and Dityrosine Formation of the Alzheimer's Disease Amyloid-β Peptide. Biochemistry-Us. 2007; 46:2881–2891.(d) Watanabe S, Nagano S, Duce J, Kiaei M, Li Q-X, Tucker SM, Tiwari A, Brown RH, Beal MF, Hayward LJ, Culotta VC, Yoshihara S, Sakoda S, Bush AI. Increased affinity for copper mediated by cysteine 111 in forms of mutant superoxide dismutase 1 linked to amyotrophic lateral sclerosis. Free Radical Biol. Med. 2007; 42:1534–1542. [PubMed: 17448900] (e) Barnham KJ, Bush AI. Metals in Alzheimer's and Parkinson's Diseases. Curr. Opin. Chem. Biol. 2008; 12:222–228. [PubMed: 18342639]
4. (a) Guilloreau L, Combalbert S, Sournia-Saquet A, Mazarguil H, Faller P. Redox Chemistry of Copper–Amyloid-β: The Generation of Hydroxyl Radical in the Presence of Ascorbate is Linked to Redox-Potentials and Aggregation State. Chembiochem. 2007; 8:1317–1325. [PubMed: 17577900] (b) Faller P. Copper and zinc binding to amyloid-β: coordination, dynamics, aggregation, reactivity and metal-ion transfer. Chembiochem. 2009; 10:2837–2845. [PubMed: 19877000] (c) Hureau C, Faller P. Abeta-mediated ROS production by Cu ions: structural insights, mechanisms and relevance to Alzheimer's disease. Biochimie. 2009; 91:1212–1217. [PubMed: 19332103]
5. (a) Masters R CLC, Barnham KJ, Villemagne VL. Molecular mechanisms for Alzheimer’s Disease: Implications for neuroimaging and therapeutics. J. Neurochem. 2006; 97:1700–1725. [PubMed: 16805778] (b) Terry RDM, Salmon E, et al. Physical basis of cognitive alterations in Alzheimer’s disease: synapse loss is the major correlate of cognitive impairment. Annals of Neurology. 1991; 30:572–580. [PubMed: 1789684]
6. Cohen SI, Linse S, Luheshi LM, Hellstrand E, White DA, Rajah L, Otzen DE, Vendruscolo M, Dobson CM, Knowles TP. Proliferation of amyloid-beta42 aggregates occurs through a secondary nucleation mechanism. Proceedings of the National Academy of Sciences of the United States of America. 2013
7. Faller P, Hureau C, Dorlet P, Hellwig P, Coppel Y, Collin F, Alies B. Methods and techniques to study the bioinorganic chemistry of metal–peptide complexes linked to neurodegenerative diseases. Coordin Chem Rev. 2012; 256:2381–2396.
8. Perez LR, Franz KJ. Minding metals: tailoring multifunctional chelating agents for neurodegenerative disease. Dalton Trans. 2010; 39:2177–2187. [PubMed: 20162187]
9. (a) Lincoln KM, Gonzalez P, Richardson TE, Julovich DA, Saunders R, Simpkins JW, Green KN. 'A potent antioxidant small molecule aimed at targeting metal-based oxidative stress in neurodegenerative disorders. Chem. Commun. 2013; 49:2712–2714.(b) Lincoln KM, Richardson TE, Rutter L, Gonzalez P, Simpkins JW, Green KN. An N-heterocyclic amine chelate capable of antioxidant capacity and amyloid disaggregation. Acs Chem Neurosci. 2012; 3:919–927. [PubMed: 23173072]

10. (a) Di Stefano A, Sozio P, Cocco A, Iannitelli A, Santucci E, Costa M, Pecci L, Nasuti C, Cantalamessa F, Pinnen F. L-Dopa- and dopamine-(R)-alpha-lipoic acid conjugates as multifunctional codrugs with antioxidant properties. J Med Chem. 2006; 49:1486–1493. [PubMed: 16480285] (b) Krishnan CV, Garnett M. Electrochemical Behavior of the Super Antioxidant, alpha-Lipoic Acid. Int J Electrochem Sc. 2011; 6:3607–3630.(c) Shay KP, Moreau RF, Smith EJ, Hagen TM. Is alpha-lipoic acid a scavenger of reactive oxygen species in vivo? Evidence for its initiation of stress signaling pathways that promote endogenous antioxidant capacity. Iubmb Life. 2008; 60:362–367. [PubMed: 18409172] (d) Shu, J. Antioxidant Mechanisms of Ascorbate and (R)-Alpha-Lipoic Acid in Aging and Transition Metal Ion-Mediated Oxidative Stress. Oregon State University; 2003. (e) Smith AR, Visioli F, Frei B, Hagen TM. Lipoic acid significantly restores, in rats, the age-related decline in vasomotion. Brit J Pharmacol. 2008; 153:1615–1622. [PubMed: 18297110]

11. Ono K, Hirohata M, Yamada M. alpha-Lipoic acid exhibits anti-amyloidogenicity for beta-amyloid fibrils in vitro. Biochem Bioph Res Co. 2006; 341:1046–1052.

12. De Leon-Rodriguez LM, Kovacs Z, Esqueda-Oliva AC, Miranda-Vera AD. Highly regioselective N-trans symmetrical diprotection of cyclen. Tetrahedron Lett. 2006; 47:6937–6940.

13. (a) Alonso E, Ramon DJ, Yus M. Reductive deprotection of allyl, benzyl and sulfonyl substituted alcohols, amines and amides using a naphthalene-catalysed lithiation. Tetrahedron. 1997; 53:14355–14368.(b) Endo T, Kerman K, Nagatani N, Takamura Y, Tamiya E. Label-free detection of peptide nucleic acid-DNA hybridization using localized surface plasmon resonance based optical biosensor. Anal Chem. 2005; 77:6976–6984. [PubMed: 16255598]

14. Izatt RM, Pawlak K, Bradshaw JS, Bruening RL. Thermodynamic and kinetic data for macrocycle interactions with cations and anions. Chem. Rev. 1991; 91:1721–1785.

15. Tougu V, Karafin A, Palumaa P. Binding of zinc(II) and coppeRII) to the full-length Alzheimer's amyloid-beta peptide. J Neurochem. 2008; 104:1249–1259. [PubMed: 18289347]

16. (a) Braymer JJ, DeToma AS, Choi JS, Ko KS, Lim M-H. Recent Development of Bifunctional Small Molecules to Study Metal-Amyloid -β-Species in Alzheimer's Disease. International Journal of Alzheimer's Disease. 2011:1–9.(b) Hyung SJ, DeToma AS, Brender JR, Lee S, Vivekanandan S, Kochi A, Choi JS, Ramamoorthy A, Ruotolo BT, Lim MH. Insights into antiamyloidogenic properties of the green tea extract (-)-epigallocatechin-3-gallate toward metal-associated amyloid-beta species. Proceedings of the National Academy of Sciences of the United States of America. 2013; 110:3743–3748. [PubMed: 23426629] (c) Braymer JJ, Choi JS, DeToma AS, Wang C, Nam K, Kampf JW, Ramamoorthy A, Lim MH. Development of Bifunctional Stilbene Derivatives for Targeting and Modulating Metal-Amyloid-beta Species. Inorg Chem. 2011; 50:10724–10734. [PubMed: 21954910] (d) Hindo SS, Mancino AM, Braymer JJ, Liu YH, Vivekanandan S, Ramamoorthy A, Lim MH. Small Molecule Modulators of Copper-Induced A beta Aggregation. J Am Chem Soc. 2009; 131:16663–16665. [PubMed: 19877631]

17. Rossi L, Lombardo MF, Ciriolo MR, Rotilio G. Mitochondrial dysfunction in neurodegenerative diseases associated with copper imbalance. Neurochem Res. 2004; 29:493–504. [PubMed: 15038597]

18. Freedman JH, Ciriolo MR, Peisach J. The Role of Glutathione in Copper-Metabolism and Toxicity. J Biol Chem. 1989; 264:5598–5605. [PubMed: 2564391]

19. Richardson TE, Yang SH, Wen Y, Simpkins JW. Estrogen protection in Friedreich's ataxia skin fibroblasts. Endocrinology. 2011; 152:2742–2749. [PubMed: 21540287]

20. (a) Jomova K, Vondrakova D, Lawson M, Valko M. Metals, oxidative stress and neurodegenerative disorders. Mol Cell Biochem. 2010; 345:91–104. [PubMed: 20730621] (b) Muller A, Knaack M, Olbrich A. NMR spectroscopic characterization of isomeric S-oxides derived from alpha-lipoic acid. Magn Reson Chem. 1997; 35:111–114.

21. (a) Amaro M, Birch DJS, Rolinski OJ. Beta-amyloid oligomerisation monitored by intrinsic tyrosine fluorescence. Phys Chem Chem Phys. 2011; 13:6434–6441. [PubMed: 21373703] (b) Rolinski OJ, Amaro M, Birch DJS. Early detection of amyloid aggregation using intrinsic fluorescence. Biosens Bioelectron. 2010; 25:2249–2252. [PubMed: 20362424] (c) Khan A, Ashcroft AE, Korchazhkina OV, Exley C. Metal-mediated formation of fibrillar ABri amyloid. J Inorg Biochem. 2004; 98:2006–2010. [PubMed: 15541488]

22. (a) Chen X TW, He Y, Zhang C, Wu Z, Liao K, Wang J, Guo Z. Effects of Cyclen and Cyclam on Zinc(II)- and CoppeRII)-Induced Amyloid β-Peptide Aggregation and Neurotoxicity. Inorg Chem. 2009; 48:5801–5809. [PubMed: 19496588] (b) Schugar H, Green DE, Bowen ML, Scott LE, Storr T, Bohmerle K, Thomas F, Allen DD, Lockman PR, Merkel M, Thompson KH, Orvig C. Combating Alzheimer's disease with multifunctional molecules designed for metal passivation. Angew Chem Int Edit. 2007; 46:1716–1718.

23. Rayne S, Forest K. Performance of the ALOGPS 2.1 program for octanol-water partition coefficient prediction with organic chemicals on the Canadian Domestic Substances List. Nature Precedings. 2009

24. Karasova JZ, Jun D, Kuca K. Screening of blood-brain barrier penetration using the immobilized artificial membrane phosphatidylcholine column chromotography at the physiological pH. Mil. Med. Sci. Lett. 2013; 82:55–62.

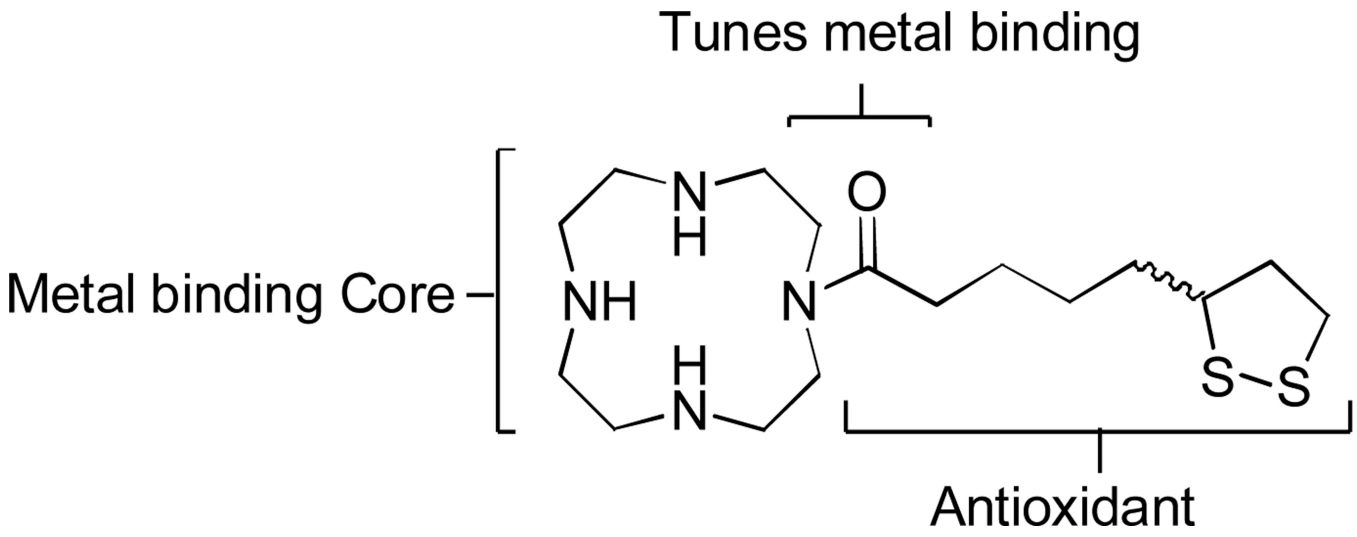

Figure 1.
Design of lipoic cyclen (**1**).

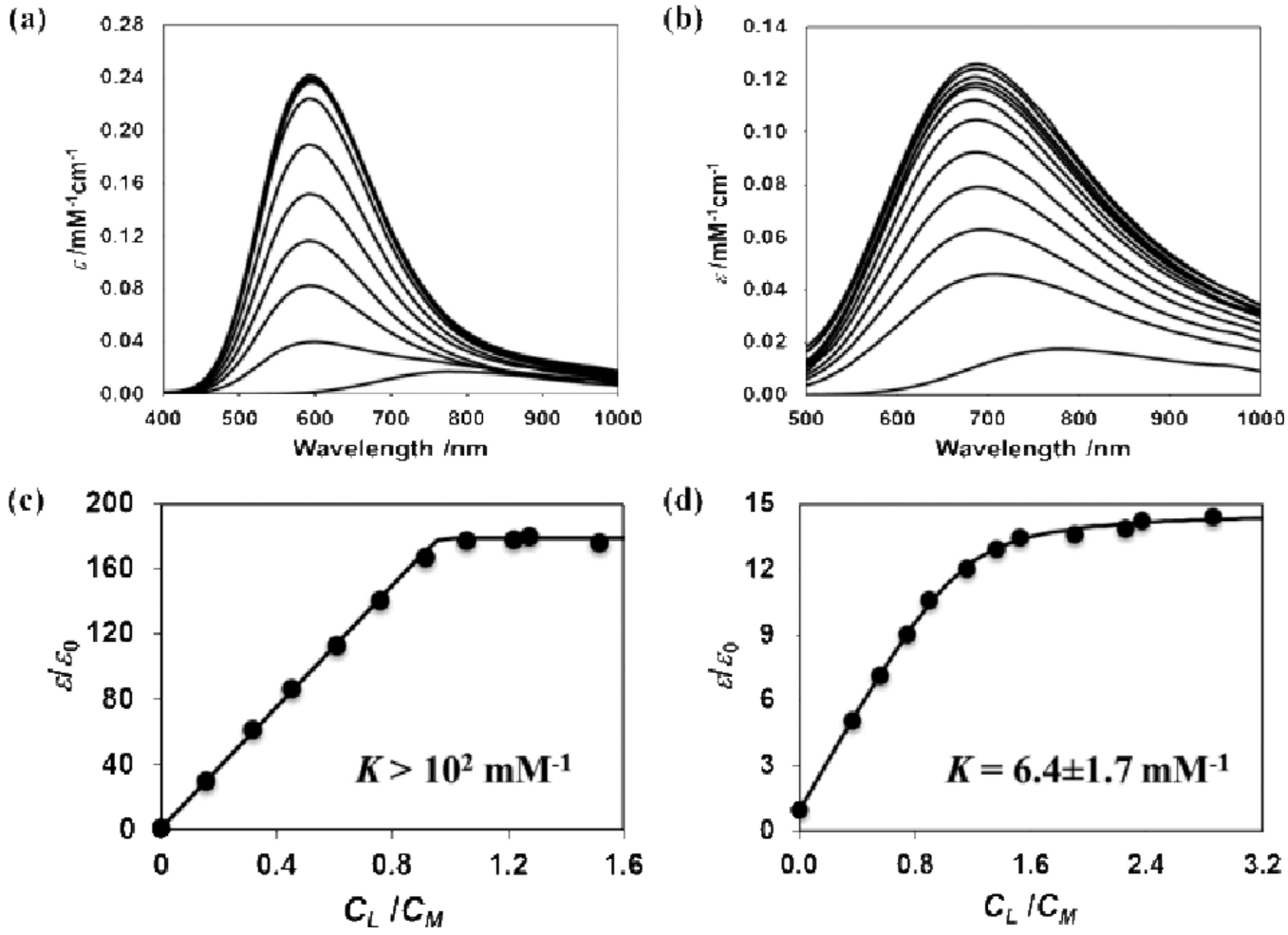

Figure 2.

Normalized absorption spectra of 3 mM copper nitrate with (a) cyclen (from 0 to 5.0 mM) and (b) **1** (from 0 to 9.0 mM), at pH=5.0 and 0.10M ionic strength. Arrows indicate increasing absorption with increasing ligand concentration. Corresponding relative change of copper absorption coefficient, $\varepsilon/\varepsilon_0$, as function of molar ratio between ligand and copper for (c) cyclen and (d) **1**. Experimental data points are shown as dark circles and the fitting function as a line.

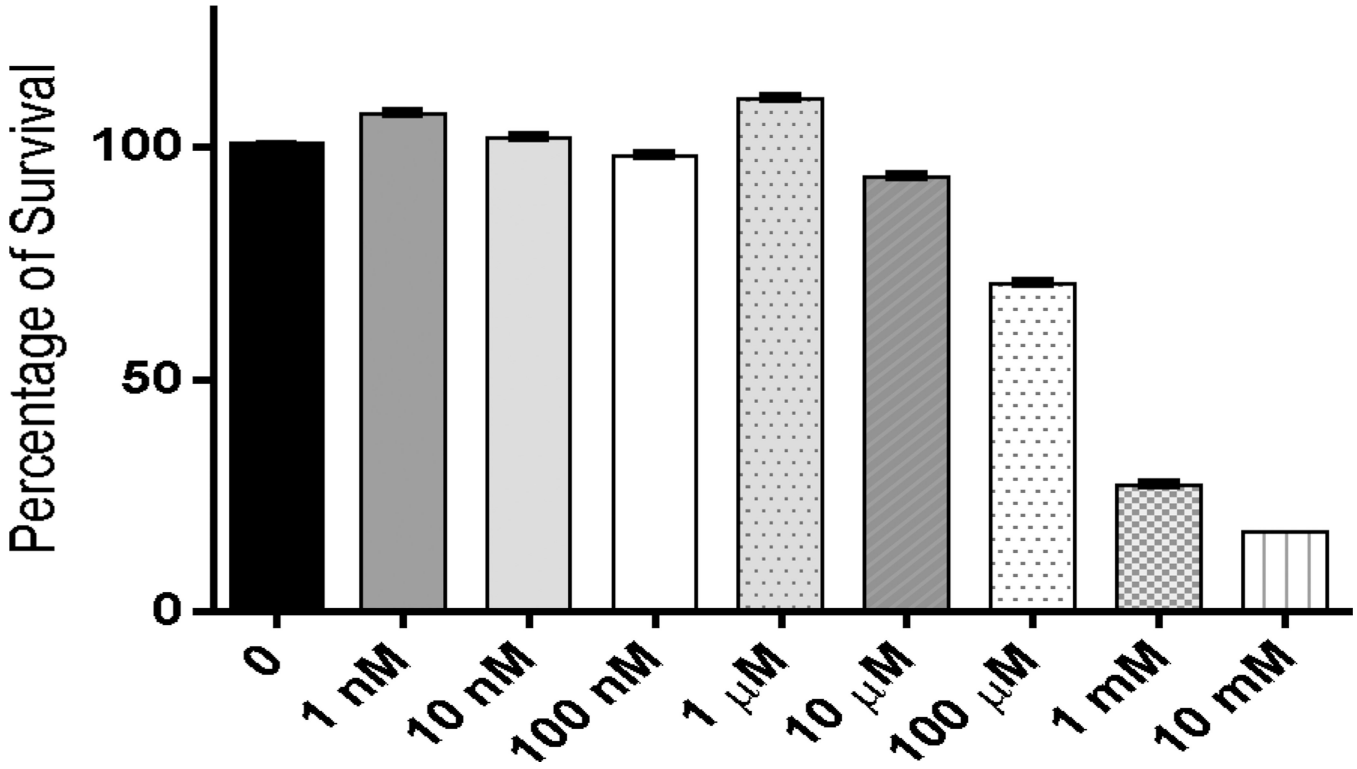

Figure 3.
Screening for biocompatibility of **1** using the MTT assay, with 10 fold dilution concentrations, in HT-22 cell line (n=8).

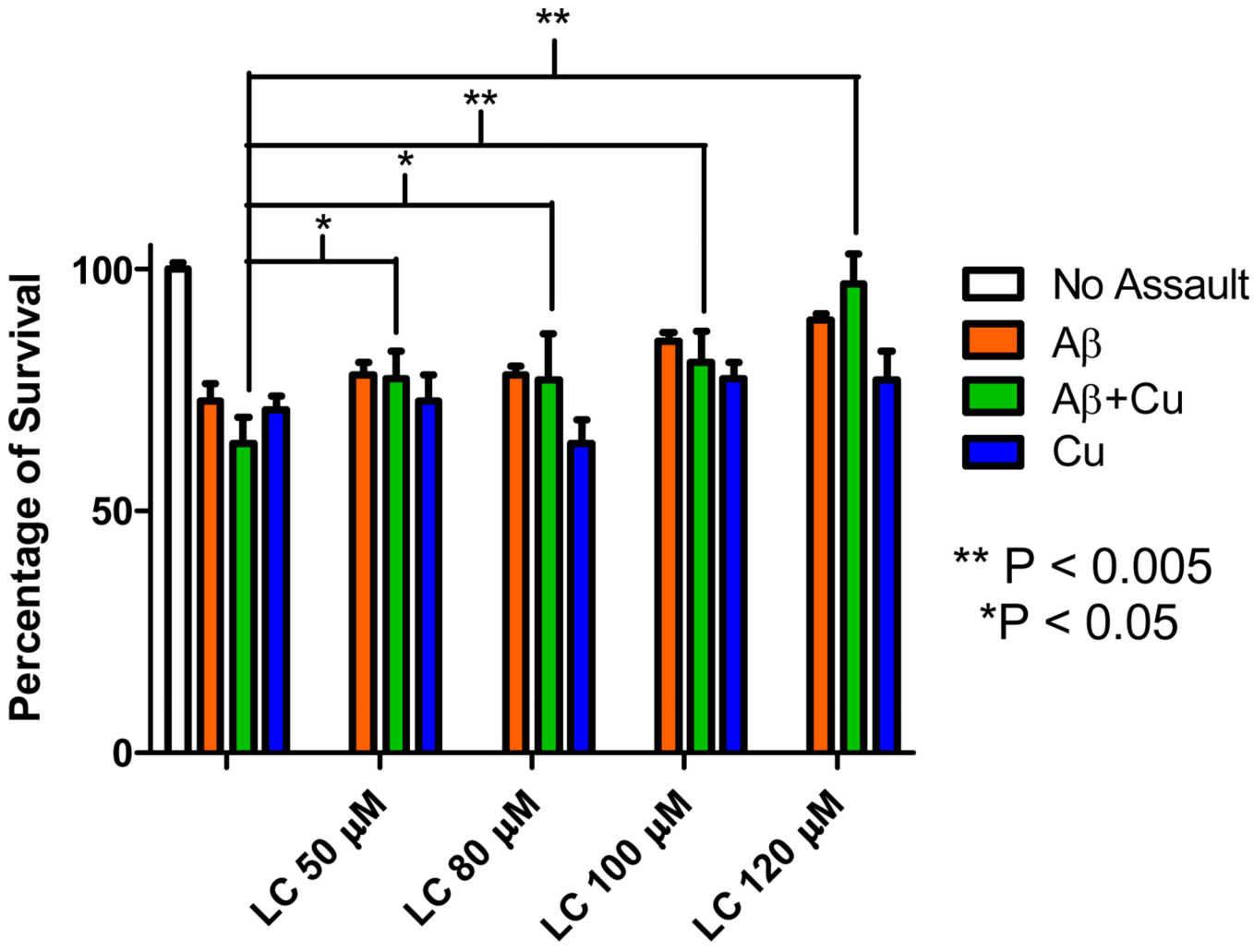

Figure 4.

Protective effect of **LC** (**1**) against copper-Aβ associated neurotoxicity in HT-22 cells in a 48 h. treatment using MTT assay. Aβ (15 μM), $CuCl_2$ (15 μM), **1** (50, 80, 100, 120 μM). Plots showing the statistical significance for Aβ and Cu^{2+} are shown in SI Figures S2 and S3.

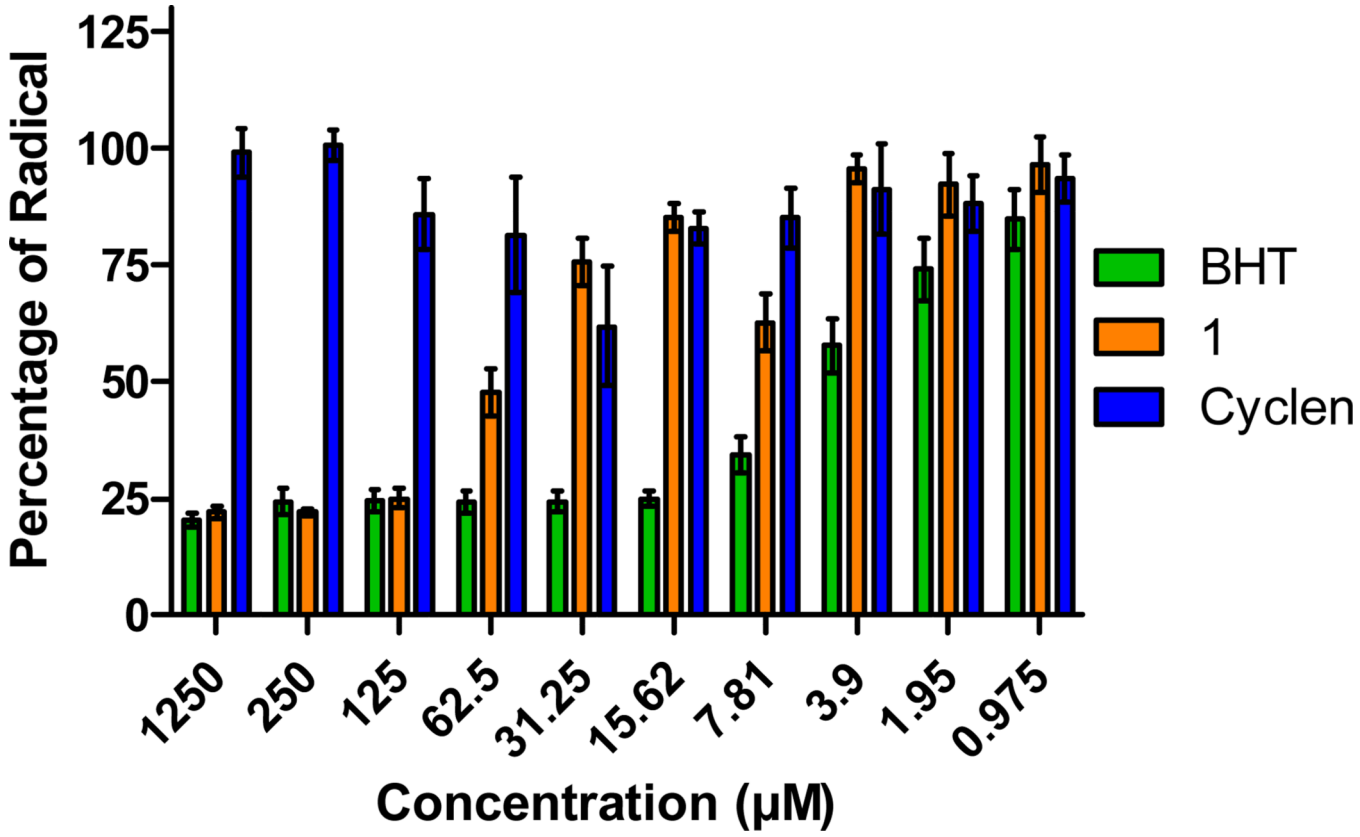

Figure 5.
Radical scavenging activity of **1** at different concentrations in comparison with the positive control and the backbone cyclen.

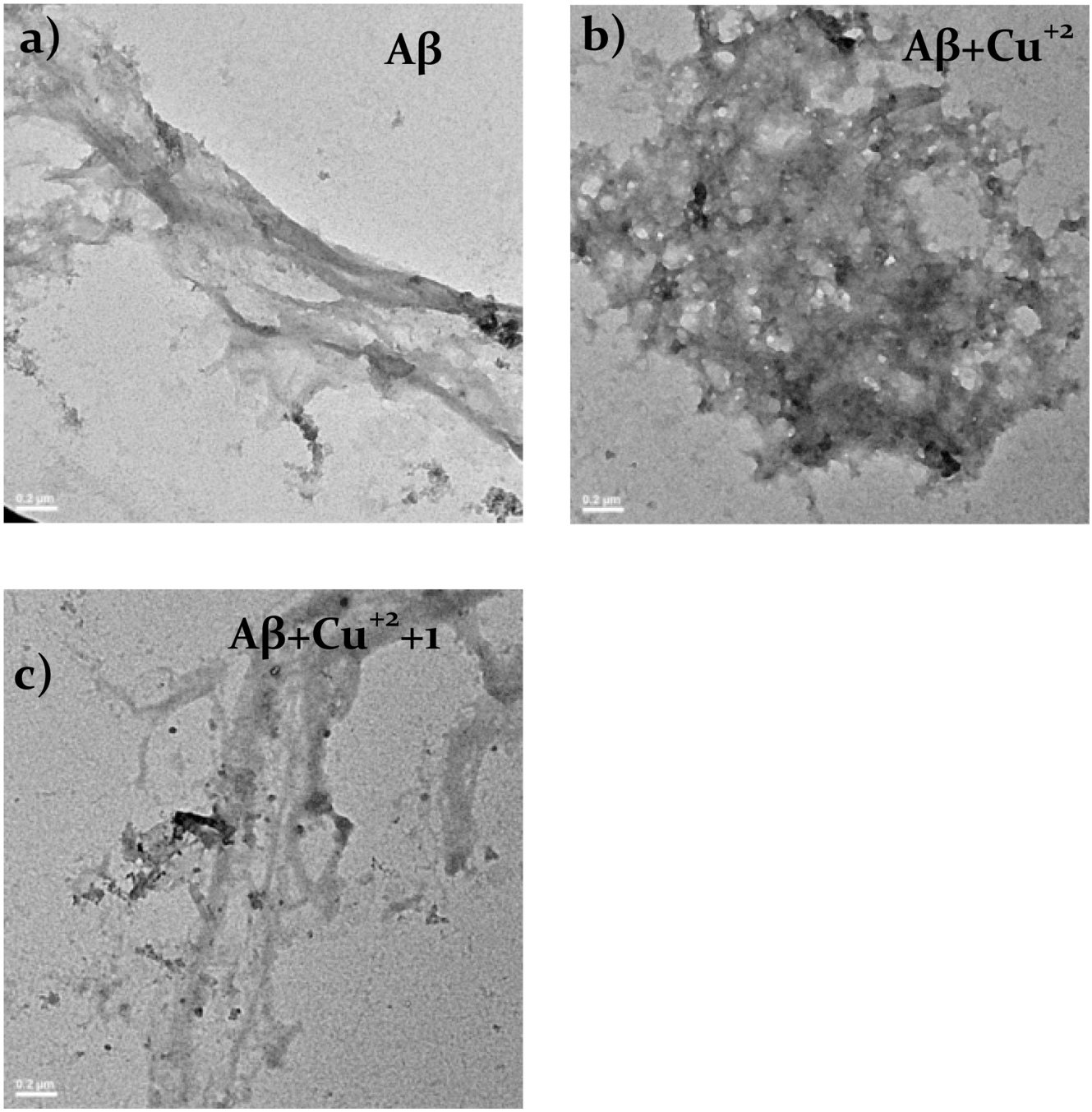

Figure 6.

TEM images of Aβ samples after incubation overnight with (a) Aβ, (b)Aβ + Cu^{2+}, (c) Aβ + Cu^{2+} + **1**. Scale bars represent 0.2 μm.

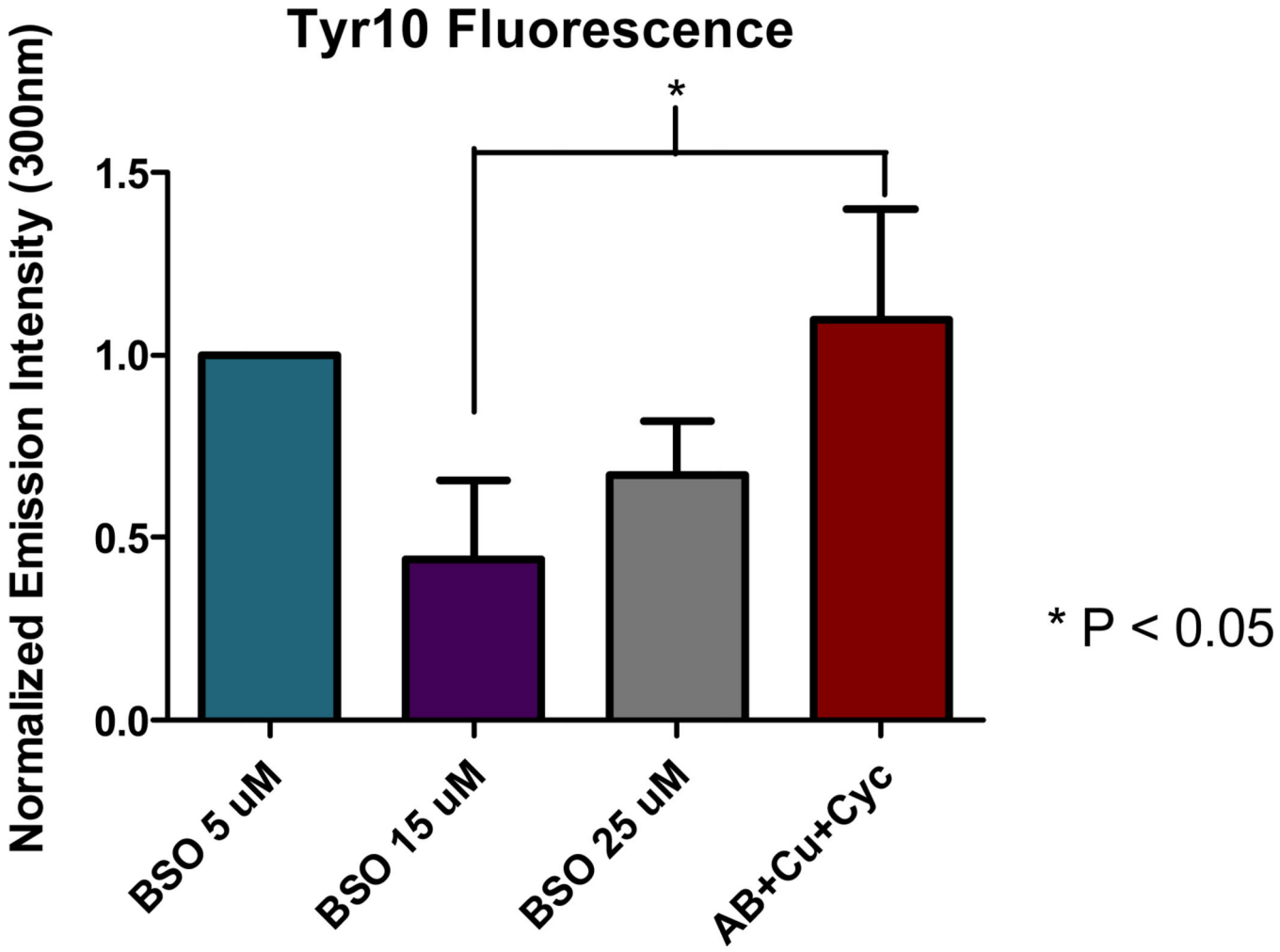

Figure 7.
Intrinsic fluorescence intensity of $A\beta_{1-40}$ in comparison with the addition of Cu^{2+}, **1** and cyclen.

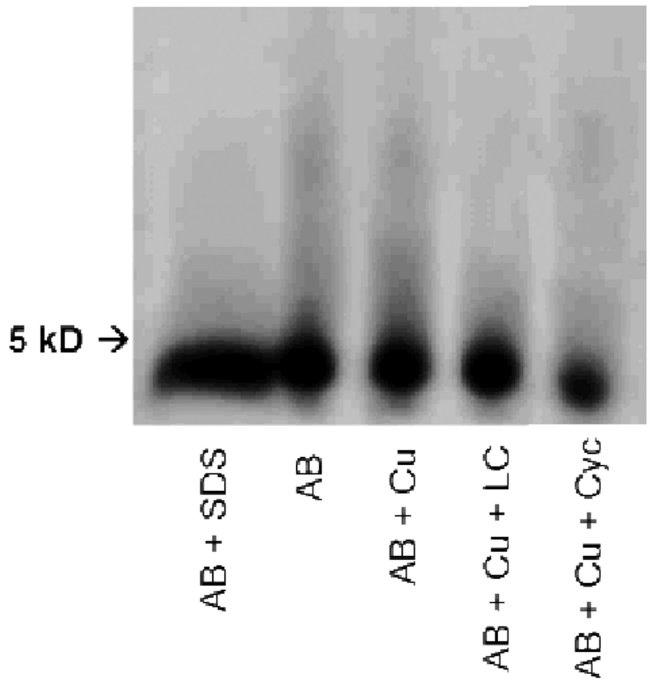

Compound	No. of pixels
Aβ	1216897
Aβ + Cu^{2+}	1212143
Aβ + Cu^{2+} + 1	1153096
Aβ + Cu^{2+} + Cyc	1237541

Figure 8.
Results of visualize native gel electrophoresis followed by western blot.

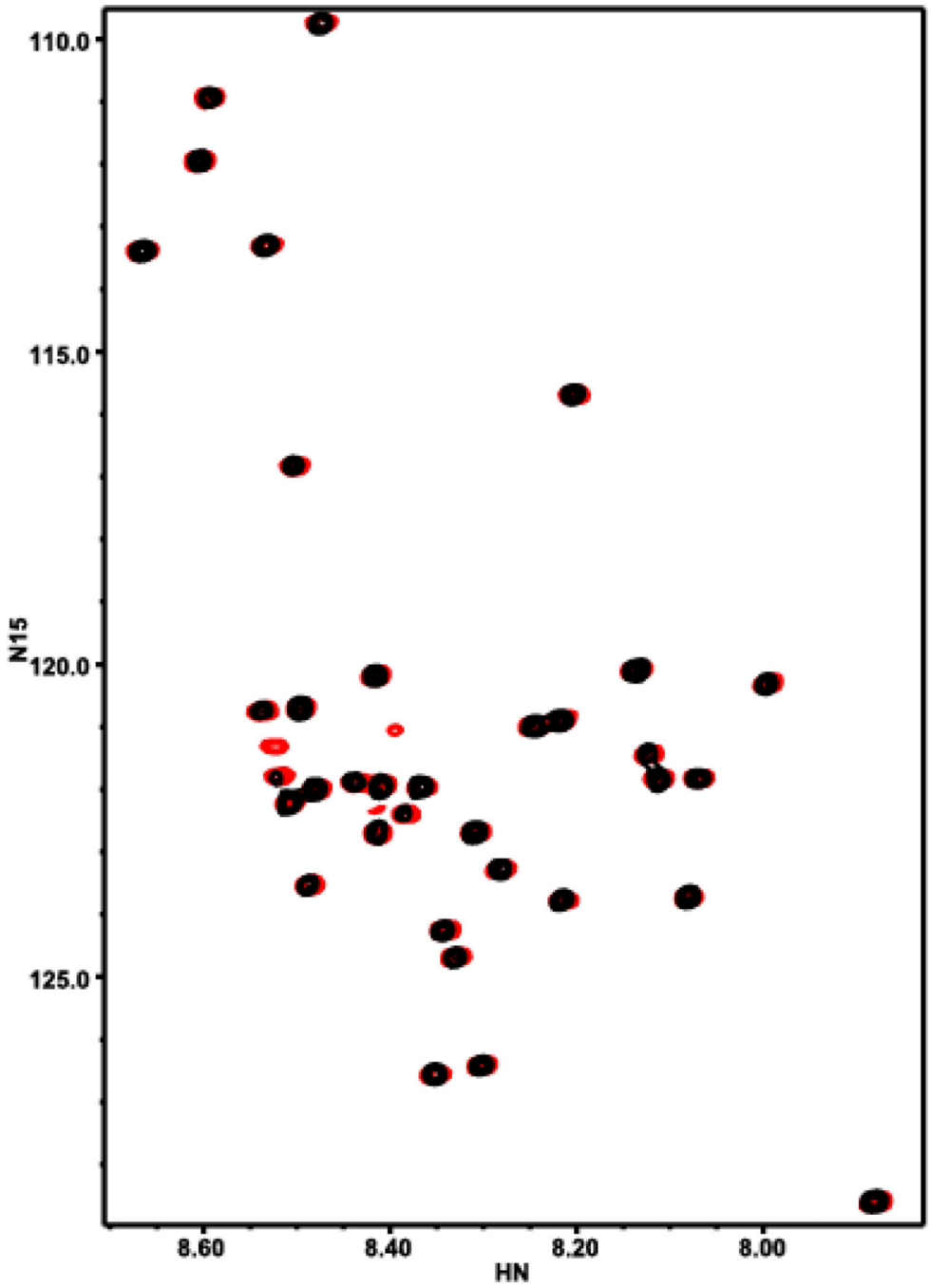

Figure 9.
Interaction of **1** with Aβ monitored by HSQC spectra: ^{15}N-A$\beta_{1–40}$ (black) and ^{15}N-A$\beta_{1–40}$ and **1** (1.5 eq.) (red).

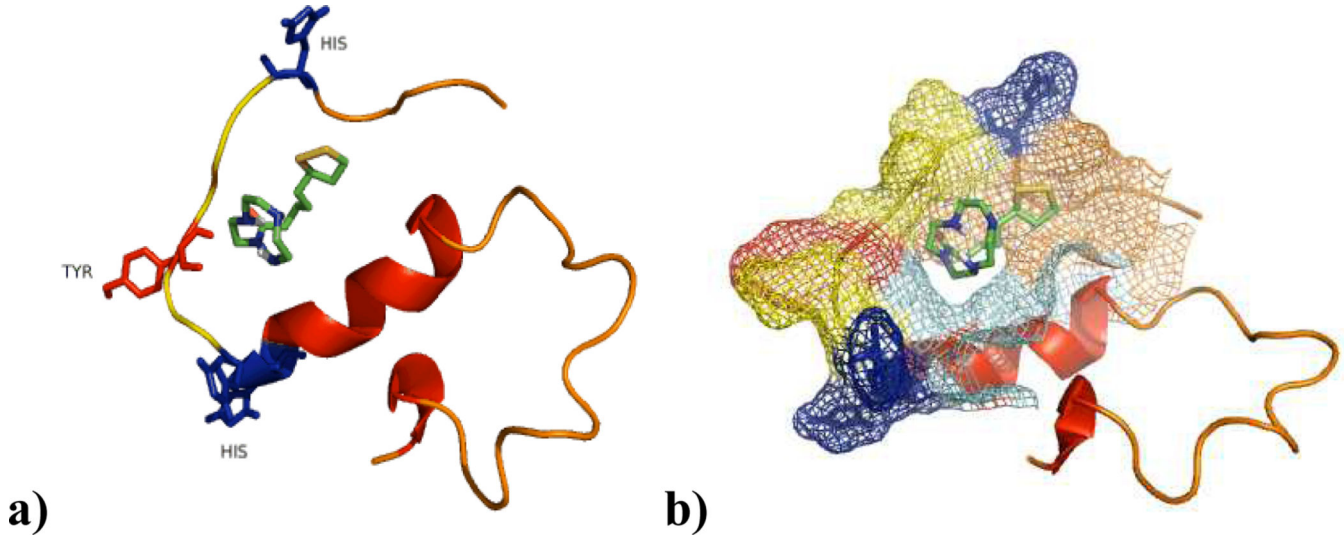

Figure 10.
Docking Studies of **1** with amyloid protein using AutoDock Vina.

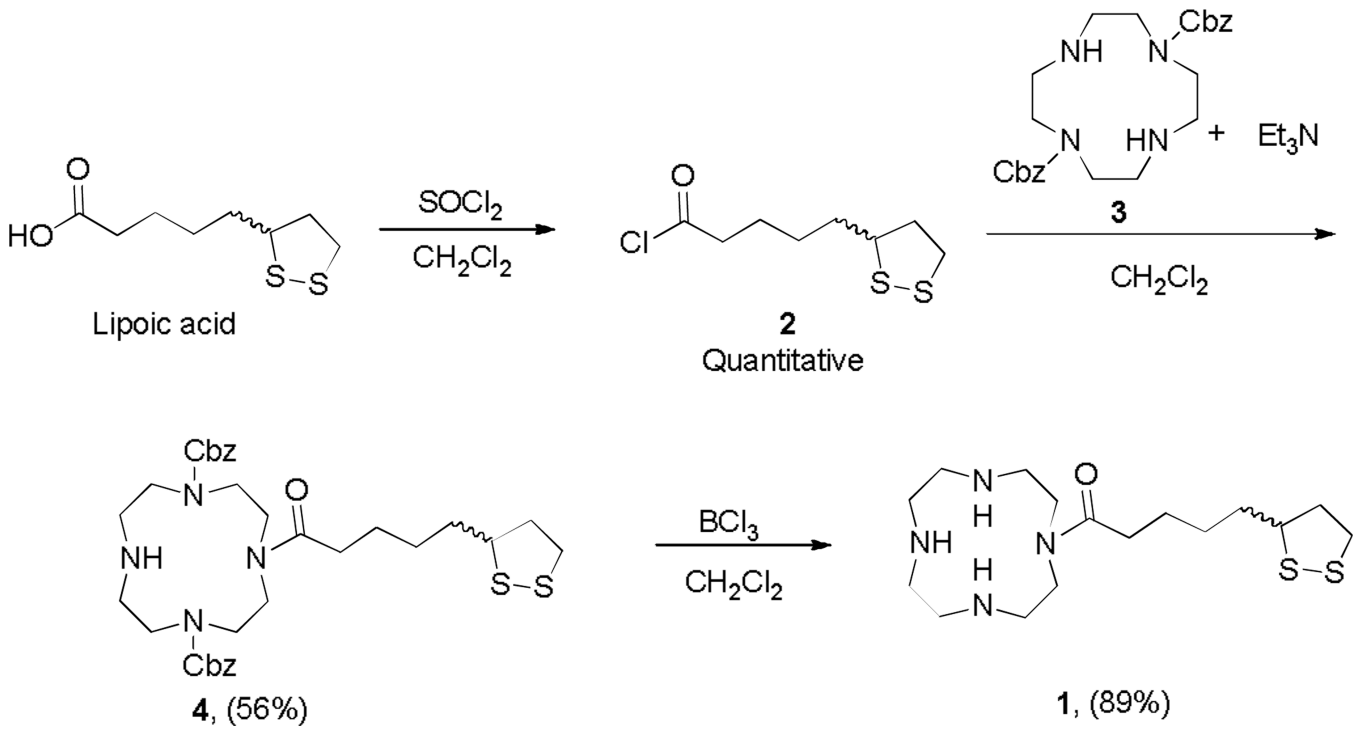

Scheme 1.
Synthetic methods used to produce **1**.

Table 1

Calculated EC_{50} values from HT-22 Neuronal and HEK-293 Cells following 48 hours of treatment with cyclen or **1** molecules determined using the MTT assay.

	EC_{50} (μM) **HT-22 neuronal**	**HEK-293 kidney**
Cyclen	81.4	132.4
1	749.1	391.9

Table 2

Calculated K_{ow} values to determine BBB permeability of **1**.

Log K_{ow} fragment description	**Coefficient**	**Value obtained for 1**
-CH2- [aliphatic carbon]	0.4911	6.8754
-CH [aliphatic carbon]	0.3614	0.3614
-NH- [aliphatic attach]	− 1.4962	−4.4886
-N< [aliphatic attach]	−1.8323	−1.8323
-C(=O)N [aliphatic attach]	−0.5236	−0.5236
-SS- [disulfide]	0.6497	0.5497
Equation Constant		0.2290
Log K_{ow}		**1.1710**